Journal of Medicinal Chemistry
Miniperspective

*J. Med. Chem.* **2010,** *53,* 933–941 **933**
DOI: 10.1021/jm901039z

# $^{18}$F Stilbenes and Styrylpyridines for PET Imaging of Aβ Plaques in Alzheimer's Disease: A Miniperspective

Hank F. Kung,*[,†,‡] Seok Rye Choi,[§] Wenchao Qu,[†] Wei Zhang,[§] and Daniel Skovronsky[†,§]

[†]*Department of Radiology and* [‡]*Department of Pharmacology, University of Pennsylvania, Philadelphia, Pennsylvania 19104, and* [§]*Avid Radiopharmaceuticals, Inc., Philadelphia, Pennsylvania 19104*

*Received July 13, 2009*

## Introduction: Alzheimer's Disease (AD)

Alzheimer's disease (AD[a]) is a neurodegenerative disease of the brain characterized by a slowly progressive dementia. This insidious disease is growing in importance because it affects millions of older patients. Clinical symptoms of AD include cognitive decline, irreversible memory loss, disorientation, and language impairment. Major neuropathology observations of post-mortem AD brain include the presence of senile plaques containing β-amyloid (Aβ) aggregates and neurofibrillary tangles containing highly phosphorylated tau proteins (Figure 1A).[1,2] Several genomic factors have been linked to AD. Familial AD (or early onset AD) has been reported to have mutations in genes encoding β-amyloid precursor protein (APP), presenilin 1, presenilin 2, and apolipoprotein E (APOE).[3] The exact mechanisms of these mutations, which lead to the development of AD, are not fully understood; however, formation of plaques comprising Aβ peptide in the brain is a pivotal event in the pathology of Alzheimer's disease. Significant evidence suggests that accumulation and aggregation of Aβ peptides may play a major causative role in AD pathogenesis.[2,4] The excessive burden of Aβ, produced by various mechanisms, may represent the starting point of neurodegenerative events and may initiate a cascade of events (β-amyloid cascade, Figure 1B) that includes gliosis, inflammatory changes, neuritic/synaptic change, tangles, and transmitter loss.[2] Currently, there is no definitive method to diagnose AD except by post-mortem evaluation and staining of the brain tissue, which demonstrates the existence of Aβ plaques.

Recent reports have suggested that β-amyloid aggregates in the brain play a key role in a cascade of events leading to AD.[2,5] Thus, the development of diagnostic imaging agents targeting Aβ aggregates is very important in the diagnosis and treatment of AD. Novel PET imaging agents specifically targeting the Aβ plaques may lead to early detection of AD pathology, differential diagnosis of patients with dementia, and monitoring of patients who are undergoing drug treatment designed to reverse the Aβ buildup in the brain.

Indeed, diagnosis and treatment of AD have been hampered by the absence of reliable noninvasive markers for the underlying pathology. Diagnosis based on consensus criteria is approximately 81% sensitive and 70% specific by comparison to the gold standard of pathology at autopsy.[6] In addition to errors of misdiagnosis in patients with AD, there is significant underdiagnosis; approximately 10% of community dwelling elderly still have undiagnosed dementia, and community physicians may fail to diagnose up to 33% of mild dementia cases.[7] Thus, there is a need for a biomarker that can be applied in the community setting and can help physicians separate those patients who do not have AD from those who have pathological signs and should be evaluated further. Additionally, there are a large number of patients who, upon comprehensive diagnostic testing, are found to have cognitive impairment but are not demented and thus do not meet diagnostic criteria for AD (e.g., patients with mild cognitive impairment, MCI). Some, but not all, of these patients will go on to develop AD within 3−5 years. A reliable biomarker might aid prognostic evaluation by documenting the presence or absence of AD related pathology.

On the basis of the definitions of AD endorsed by the American Academy of Neurology, American Psychiatric Association (DSM-IV), and others, patients without abnormal amyloid plaque levels do not meet currently accepted neuropathological criteria for AD. This definition of AD, which includes amyloid plaques as a required feature, is supported by more than 100 years of autopsy data. Therefore, on the basis of this widely endorsed definition of AD, the use of a test for ruling out the presence of amyloid plaque pathology in subjects with clinical signs and symptoms of cognitive impairment will effectively rule out the diagnosis of AD and lead to more careful evaluation and appropriate treatment for alternative causes of cognitive deficits. Moreover, the use of a test for ruling in the presence of abnormal levels of Aβ plaques in the brain of subjects with signs and symptoms of cognitive impairment will lead to the selection of patients who warrant more detailed workup for the possible diagnosis of AD or MCI.

The differential diagnosis for AD includes a large number of other diseases. At early stages of disease (e.g., MCI), frequent confounds include cognitive impairment as a result of underlying depression, effects of CNS active medications,

*To whom correspondence should be addressed. Phone: (215) 662-3096. Fax: (215) 349-5035. E-mail: kunghf@gmail.com.

[a] Abbreviations: AD, Alzheimer's disease; Aβ, β-amyloid; FPEG, fluoro-pegylation; APOE, apolipoprotein E; APP, β-amyloid precursor protein; MCI, mild cognitive impairment; FTLD, temporal lobar dementia; DLB, Lewy bodies; CJD, Creutzfeld−Jacob disease; SPECT, single photon emission computed tomography; PET, positron emission tomography; FDG, 2-fluoro-2-deoxyglucose; CG, chrysamine G; PIB, Pittsburgh compound B; FDDNP, 2-(1-{6-[(2-$^{18}$F-fluoroethyl)-(methyl)amino]-2-naphthyl}ethylidene)malononitrile; IMPY, 6-[iodo-2-(4′-*N*,*N*-dimethylamino)phenylimidazo[1,2-*a*]pyridine; SB-13, 4-*N*-methylamino-4′-hydroxystilbene.



Published on Web 10/21/2009

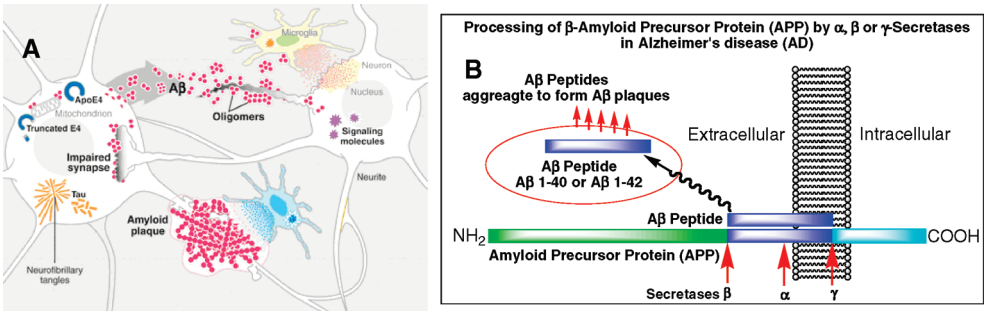


**Figure 1.** (A) Processes ($\beta$-amyloid cascade) participating in AD pathogenesis. A$\beta$ peptides produced by neurons aggregate into a variety of assemblies, some of which may impair synapses and neuronal dendrites. Build-up of pathogenic A$\beta$ aggregates could result from increased production or aggregation or from deficient clearance mechanisms. This multifactorial scenario leads to progressive disintegration of neural circuits, isolation and loss of neurons, network failure, and neurological decline. (From Roberson, E. D.; Mucke, L. 100 years and counting: prospects for defeating Alzheimer's disease. *Science* 2006, *314*, 781−784.[2] Reprinted with permission from AAAS. Copyright 2006 AAAS.) (B) Simplified model of excessive A$\beta$ production leading to Alzheimer's disease (AD). Normally, amyloid precursor protein (APP) is metabolized by at least three proteases ($\alpha$-, $\beta$-, and $\gamma$-secretases). A$\beta$-Peptides are produced by $\beta$-secretase, cleaving at the N-terminal residue, and by $\gamma$-secretase, cleaving at the C-terminal residue of APP. The fibrillar aggregates of amyloid peptides, A$\beta$40 and A$\beta$42, are the major constituents of senile plaques in AD patients. The A$\beta$ aggregates are believed to be responsible for initiating a cascade of events leading to neurotoxicity and AD.

**Table 1.** Useful Radionuclides for Single Photon Emission Computed Tomography (SPECT) and Positron Emission Tomography (PET)

| | half-life $T_{1/2}$ | mode of decay (keV) |
|---|---|---|
| | PET | |
| $^{11}$C | 20 min | 511 ($\beta^+$) |
| $^{18}$F | 110 min | 511 ($\beta^+$) |
| $^{68}$Ga | 68 min | 511 ($\beta^+$) |
| | SPECT | |
| $^{123}$I | 13 h | 159 |
| $^{99m}$Tc | 6 h | 140 |

inadequately treated or end stage medical conditions affecting other organ systems, and even normal age-related changes. At later stages of disease, more common confounds include vascular dementia, frontal temporal lobar dementia (FTLD) complex, dementia with Lewy bodies (DLB), as well as rarer neurodegenerative diseases such as Creutzfeld−Jacob disease (CJD). Importantly, AD subjects will always have A$\beta$ plaques, whereas amyloid is seen not at all or only sporadically in most of these other diseases. In each case, appropriate prognosis and treatment require accurate diagnostic assessment.

## Current Status of PET and SPECT Imaging of Patients with Alzheimer's Disease

There are two types of nuclear medicine imaging devices: single photon emission computed tomography (SPECT) and positron emission tomography (PET). The radionuclides useful for imaging are based on the physical characteristics of different isotopes: half-lives and mode of decay (emitting single photons or a positron subsequently annihilating with a neighboring electron to emit two 511 keV photons at 180° apart, Table 1).

A wealth of literature in using PET and SPECT for measuring changes in regional glucose metabolism and blood flow with aging and dementia has been reported.[8] One example is the use of PET imaging with [$^{18}$F]2-fluoro-2-deoxyglucose (FDG), which has been shown to improve the routine clinical diagnosis of suspected AD;[9] however, FDG/PET cannot measure the defining pathogenic lesion in AD, the presence of A$\beta$ aggregates in the brain. Other anatomical imaging studies, such as MRI, provide detailed structural information on the brain volume, and regional changes; however, the information is more valuable when combined with other functional studies.

## PET and SPECT A$\beta$ Plaque-Specific Imaging Agents: Benzothiazole Derivatives (PIB and AZD2184) and Other Core Structures

Development of A$\beta$ plaque-specific imaging agents (based on a 2-phenylbenzothiazole core) has been extensively reported and reviewed previously.[10−12] One of the essential prerequisites for a successful imaging agent for A$\beta$ plaques in the brain is the ability to rapidly penetrate the intact blood−brain barrier. A small and moderately lipophilic tracer exhibiting an excellent initial brain uptake is a critical precondition, which must be met prior to any further consideration. An imaging agent is usually injected once via iv, and there is no multiple dosing like therapeutic drugs. Biodistribution study of a potential imaging agent injected intravenously in mice is often used as a test to measure the brain uptake (ability to penetrate intact blood−brain barrier). Not only should the agent have a high initial brain uptake ($>5\%$dose/g at 2 min post iv injection) but it should also have fast washout kinetics from the normal brain ($<2\%$ dose/g, at 30 min). These are highly desirable properties for a useful brain-imaging agent targeting A$\beta$ plaques.[13−15] Further evaluation of brain penetration and fast washout from normal brain tissue is often demonstrated in normal monkey by microPET imaging of brain uptake and washout. An attractive combination of a high binding affinity to the A$\beta$ plaque and fast kinetics for washout from normal brain is highly desirable in providing specific PET imaging signals. Many reported A$\beta$ plaque-targeting ligands, despite their high binding affinities, do not penetrate the brain; or once they enter the brain, the nonspecific binding is so high that it makes it impossible for the agents to offer suitable specific signals of A$\beta$ plaques.[16−18] Other technical issues including the ease of radiolabeling and in vivo and in vitro stability will also play important roles in the success or failure of the imaging agents.

Many of the approaches are based on labeling of highly conjugated dyes, such as Congo red and chrysamine G (CG), **1**.[19] Thioflavins S and T, **2**, have also been used in fluorescent staining of plaques and tangles in post-mortem AD brain

**Table 2.** Inhibition Constant[a] ($K_i$, nM) of Various Agents against Binding of **10**, [$^{18}$F]AV-45, to A$\beta$ Plaques in Post-Mortem AD Brain Homogenates (Adapted from Previously Published Data[22])[b]

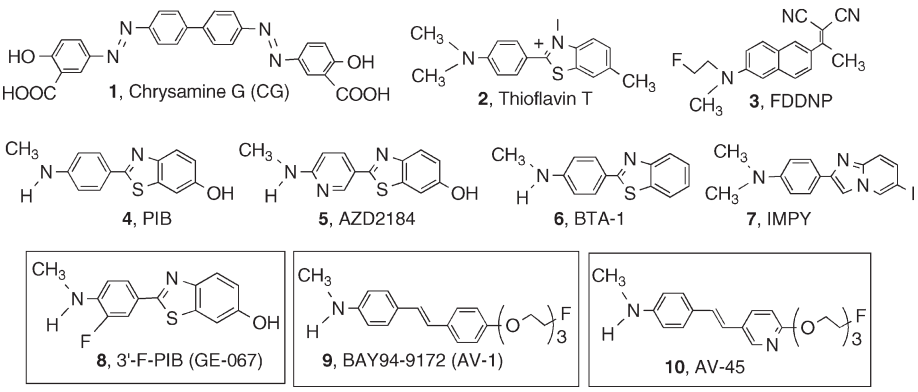


| compd | $K_i$ (nM, $n$ = 3) | compd | $K_i$ (nM, $n$ = 3) |
|---|---|---|---|
| **1**, chrysamine G (CG) | > 1000 | **6**, BTA-1 | 1.28 ± 0.46 |
| **2**, thioflavin T | > 1000 | **7**, IMPY | 1.29 ± 0.46 |
| **3**, FDDNP | 172 ± 18 | **8**, GE-067 (3′-F-PIB) | 0.74 ± 0.38 |
| **4**, PIB | 0.87 ± 0.18 | **9**, BAY 94-9172 (AV-1) | 2.22 ± 0.54 |
| **5**, AZD2184 | 1.70 ± 0.54 | **10**, AV-45 | 2.87 ± 0.17 |

[a] Competitive binding assays were carried out in AD brain homogenates (20−25 $\mu$g), $^{18}$F-AV-45 (0.04−0.06 nM diluted in PBS) and 100 $\mu$L of competing compounds ($10^{-5}$-$10^{-10}$ M diluted serially in PBS containing 0.1% bovine serum albumin) in a final volume of 0.5 mL. Nonspecific binding was defined in the presence of BTA-1,**6**, (8 $\mu$M).[22] [b] Three $^{18}$F tracers targeting A$\beta$ aggregates (**8**, GE-067; **9**, BAY 94-9172, and **10**, AV-45) are currently under commercial development (see compounds in boxes).

sections. While such dyes have great utility for fluorescent microscopy, they are unsuitable for in vivo human imaging. Unlike histological dyes, in vivo imaging agents must effectively cross the blood−brain barrier (therefore, small lipophilic molecules are favored), should bind with much higher avidity (allowing utilization of tracer doses), and should show higher selectivity, since during microscopy but not during in vivo imaging different lesions can be distinguished by subcellualr localization or morphology (e.g., thioflavin stains both tangles and plaques, but these can be easily distinguished under the microscope). This Miniperspective will concentrate on the efforts leading to the development of stilbenes and styrylpyridines series of ligands for imaging A$\beta$ plaques in the brain. However, in the following section a general review of agents, which have been successfully tested in humans, will be presented.

A highly lipophilic tracer, [$^{18}$F]FDDNP (**3**), for binding to both tangles and plaques has been reported. PET imaging studies in humans suggest that [$^{18}$F]FDDNP shows a higher retention in regions of brain suspected of having tangles and plaques.[12] It is important to point out that [$^{18}$F]FDDNP binds to both tangles (tau aggregates) and plaques (A$\beta$ aggregates); therefore, it is not for selectively measuring A$\beta$ burden in the AD brain.

A small, neutral, and lipophilic 2-phenylbenzothiazole derivative, **4**, [$^{11}$C]6-OH-BTA-1 (PIB, often called "Pittsburgh compound B"), is the most well characterized PET imaging agent for A$\beta$ plaques in the brain. It exhibits an excellent brain penetration and initial brain uptake and displays a high binding affinity to A$\beta$ plaques ($K_i$ = 0.87 ± 0.18 nM; see Table 1).[15] In the past few years, successful PET imaging study in thousands of AD patients with [$^{11}$C]PIB has been reported.[20]

Another leading A$\beta$ plaque-targeting agent derived from a benzothiazole ring system (containing a 2-pyridinyl group instead of 2-phenyl), AZD2184 (**5**) (see Table 1), has been reported recently.[21] It is a close analogue of [$^{11}$C]PIB, **4**. It displays a high affinity for amyloid fibrils (mainly composed of A$\beta$ aggregates) in vitro. In vivo autoradiography studies showed that [$^{11}$C]AZD2184, **5**, exhibits a high signal-to-background ratio in post-mortem brain sections from AD patients.[21] Preliminary human PET imaging studies suggest that this analogue of PIB displayed fast brain kinetics and an excellent contrast for A$\beta$ plaques in the brain of AD patients. The clinical application is limited compared to that of [$^{11}$C]PIB, **4**.

The success in using $^{11}$C labeled tracer for imaging A$\beta$ plaques in the brain of suspected AD patients has provided considerable impetus for further refinement of this PET imaging technique. The practical challenges of using a $^{11}$C tracer ($T_{1/2}$ = 20 min) on a routine basis have limited its application to major medical centers, which have sufficient resources (an on-site cyclotron and a radiochemistry team). Additional tracers labeled with $^{18}$F ($T_{1/2}$ = 110 min, 511 keV, commonly produced by a cyclotron) may be useful as PET imaging agents for detection and quantification of A$\beta$ aggregates. Logistically, $^{18}$F tracers are more likely to be prepared from an off-site cyclotron. By use of $^{18}$F tracers, the manufacturing and distribution can be centralized, which will significantly simplify the clinical application. Currently, $^{18}$F-FDG/PET has been approved for the diagnosis of cancer. There is an improving infrastructure to supply $^{18}$F-FDG by local radiopharmacies, thus circumventing the need for an on-site cyclotron in nuclear medicine clinics. As such, it is possible to decouple the cyclotron from the imaging sites, where PET/CT scanners are located. Ultimately, $^{18}$F tracers may lead to a widespread application of the scanning procedure for testing A$\beta$ plaque burden in the living human brain.

A $^{18}$F labeled PIB derivative, **8**, [$^{18}$F]3′-F-PIB (GE-067) (see Table 2), has been reported[23] and is currently under a phase II clinical trial in Europe sponsored by GE Healthcare. Preliminary PET imaging studies in AD patients suggested

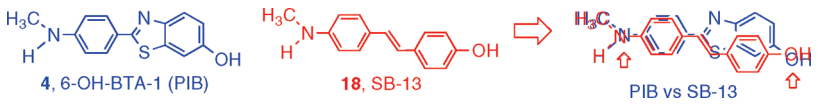


**Figure 2.** Comparison of chemical structures of **4**, PIB, and **18**, SB-13. The aromatic rings and electronically negative substitution groups, *N*-methylamino and hydroxyl (indicated by an arrow), overlap each other. In addition, both ligands are relatively planar because of the conjugating ring systems.

**Table 3.** Inhibition Constants ($K_i$, nM) of A$\beta$ Plaque-Binding Ligands

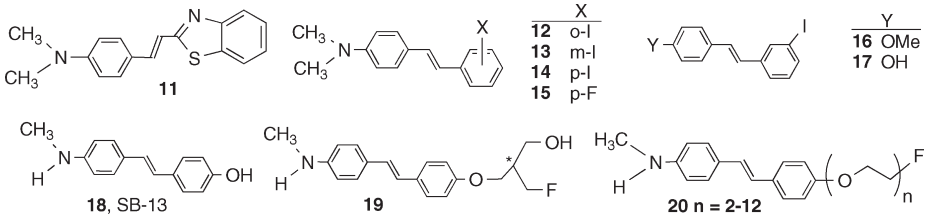


| compd | $K_i$ (nM) | compd | $K_i$ (nM) |
|---|---|---|---|
| **11** (from Aldrich) | $2.3 \pm 0.1^a$ | **16** | $22 \pm 6^a$ |
| **12** | $7.7 \pm 0.8^a$ | **17** | $32 \pm 3^a$ |
| **13** | $4.5 \pm 0.8^a$ | **18**, SB-13 | $2.4 \pm 0.2^b$ |
| **14** | $2.0 \pm 0.4^a$ | **19** | $5.0 \pm 1.2^c$ |
| **15** | $22 \pm 3^a$ | **20**, $n$ = 2−12 | See Figure 3. |

[a] Value from ref 13. [b] Value from ref 30. [c] Value from ref 18.

that this tracer is potentially useful for PET imaging of A$\beta$ plaque burden in the living human brain.[23]

Another approach of using SPECT imaging agents for mapping A$\beta$ plaque burden in the brain has also attracted a lot of attention.[24] It was reported recently that [$^{123}$I]IMPY, **7** (see Table 1), may be useful as a SPECT imaging agent targeting A$\beta$ plaques in the brain.[25] There are more SPECT scanners than PET imaging devices installed for routine clinical imaging, which provides a certain advantage of using SPECT imaging agents. Preliminary clinical data of [$^{123}$I]IMPY, **7**, in normal and AD patients showed a distinct distribution pattern similar to that of [$^{11}$C]PIB. However, the signal-to-noise ratio for plaque labeling is not as robust as that of PIB (PIB showed a $S/N$ ratio of about 2.5, while IMPY displayed a ratio of 1.8−2.0, between 30 and 50 min after an iv injection).[26] The low contrast observed may be due to the fast brain and plasma clearance observed in AD and in normal subjects. But the rapid in vivo metabolism and instability of [$^{123}$I]IMPY may have led to less than optimal signal-to-noise ratios for targeting A$\beta$ plaques in the brain. Additional candidates are being explored for SPECT imaging of A$\beta$ plaques in the brain.[24] The progress in developing SPECT imaging agents targeting A$\beta$ plaques is less advanced than that of PET imaging agents. [$^{125}$I]IMPY, **7**, is often used for in vitro binding assays to measure the inhibition constant ($K_i$) for binding to A$\beta$ aggregates. A related benzothiazole, [$^3$H]BTA-1, **6**, is also used as a ligand for in vitro binding assays.[10]

## PET Imaging Agents Based on Stilbene and Styrylpyridine

It was recognized that the chemical structures of benzothiazoles (PIB analogues) and stilbenes (SB-13 analogues) are similar; both have a highly conjugated aromatic ring system. They are relatively planar molecules, an important attribute for insertion between the $\beta$-sheets of A$\beta$ aggregates. Another common feature is an electron donating group (*N*-methylamine or hydroxyl group) at each end of the molecule.[13] They appear to compete for similar binding sites on the A$\beta$ aggregates (Figure 2).

The rigid structures of stilbene and styrylpyridine have provided core structures for developing many specific imaging agents for A$\beta$ plaques.[14,17,18,27,28] The first example of a series of stilbenes as probes for binding to A$\beta$ aggregates was published in 2001.[13] The binding affinities of stilbene derivatives **11**−**17** are excellent, as listed in Table 3. One particular stilbene derivative, [$^3$H]SB-13, **18** (Table 3, Figure 2), also showed excellent binding affinity to post-mortem AD brain tissue homogenates ($K_d = 2.4 \pm 0.2$ nM).[29,30] In vivo human PET imaging studies with [$^{11}$C]SB-13, **18**, demonstrated potential usefulness in detecting A$\beta$ plaques in the brain. To further improve the availability of PET imaging with $^{18}$F labeled agents as a tool for diagnosis of AD, a series of fluorinated stilbenes were synthesized and tested. It is not a trivial and simple exercise to add a fluorine atom to the side chain for labeling while maintaining the desired binding affinity to A$\beta$ plaques and brain penetrability. Initial attempts on developing $^{18}$F labeled SB-13, **18**, by adding a fluoroalkyl substitution group on either end of the stilbene core were met with little success. These stilbene derivatives, and likewise many other newly reported imaging agents, were too lipophilic and showed high nonspecific binding in the normal brain.

To develop a $^{18}$F labeled PET imaging agent targeting A$\beta$ plaques in the brain, two approaches were employed to reduce the lipophilicity of stilbenes.[17,18,31] One successful attempt was made using a 2-fluoromethyl-1,3-propylenediol group, **19**, and another using a fluoro-pegylation (FPEG) group, **20**, at one end of the phenyl group (see Table 3). Among them, **19** displayed a high binding affinity in post-mortem AD brain homogenates ($K_i = 5.0 \pm 1.2$ nM). The compound was successfully labeled with fluorine-18 to produce [$^{18}$F]**19**. This neutral and lipophilic tracer showed a moderate log $P$ of 2.95. In vivo biodistribution of [$^{18}$F]**19** in normal mice exhibited excellent brain penetration and rapid washout after an iv injection (4.66 and 0.33% dose/g in the brain at 2 and 60 min

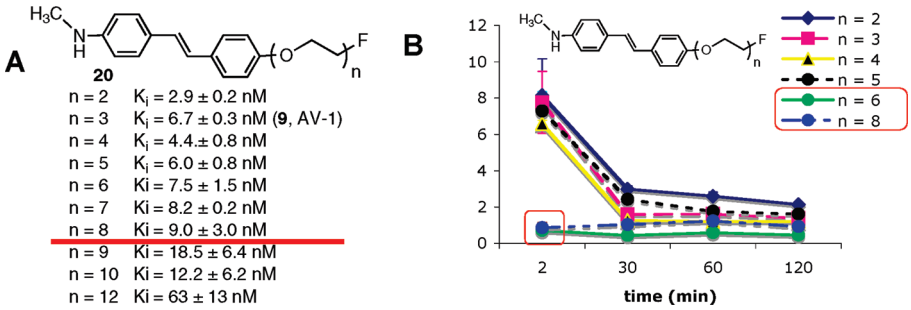


**Figure 3.** (A) Inhibition constants ($K_i$, nM) of [$^{125}$I]IMPY binding to A$\beta$ aggregates of AD brain homogenates and brain uptake in normal mice. Values ($K_i$, nM) are the mean ± SEM of three independent experiments, each in duplicate.[18] The in vitro binding data suggest that when $n < 8$, **20**, the high binding affinity was maintained ($K_i < 10$ nM) (as indicated by the red line). However, when $n$ was above and beyond 8, the binding affinity showed a significant reduction. It is noted that for this series of compounds the binding data for AV-1, **9** ($K_i$ = 6.7 nM), was slightly different from the $K_i$ value obtained later in Table 2 ($K_i$ = 2.22 nM). (B) The $^{18}$F labeled **20** ($n$ = 2−8) was injected (iv) into normal mice, and the brain uptake (% dose/g) was measured. It was surprising to find that when $n > 5$, there was a significant drop-off of brain penetration (red boxes). Comparable brain uptake of [$^{11}$C]PIB and [$^{125}$I]IMPY in mice was observed: 7 and 7.2 % dose/g at 2 min and 0.6 and 0.65% dose/g in mice at 30 min, respectively.[15,34]

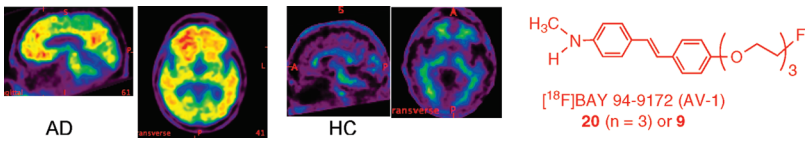


**Figure 4.** PET imaging of a healthy control (HC) and an AD patient (AD) at 70−90 min after a dose of 7 mCi of [$^{18}$F]Bay 94-9172 (AV1), **9**. Significant uptake in the frontal cortex region of AD patients was observed, while the uptake in the normal controls showed low or no uptake. (Reprinted from *The Lancet Neurology* (http://www.sciencedirect.com/science/journal/14744422), Vol. *7*; Rowe, C. C.; Ackerman, U.; Browne, W.; Mulligan, R.; Pike, K. L.; O'Keefe, G.; Tochon-Danguy, H.; Chan, G.; Berlangieri, S. U.; Jones, G.; Dickinson-Rowe, K. L.; Kung, H. P.; Zhang, W.; Kung, M. P.; Skovronsky, D.; Dyrks, T.; Holl, G.; Krause, S.; Friebe, M.; Lehman, L.; Lindemann, S.; Dinkelborg, L. M.; Masters, C. L.; Villemagne, V. L., Imaging of amyloid beta in Alzheimer's disease with (18)F-BAY94-9172, a novel PET tracer: proof of mechanism, pp 129−135, **2008**;[35] with permission from Elsevier. Copyright 2008 Elsevier.)

postinjection, respectively), a property highly desirable for A$\beta$ plaque-specific brain imaging agents. Autoradiography of post-mortem AD brain sections confirmed the high binding signal of [$^{18}$F]**19** due to the presence of A$\beta$ plaques. However, because the fluorine containing side chain has an optical center, which may complicate the in vivo metabolism, it was decided that a stilbene containing a fluoro-pegylation (FPEG) group, **20**, which has no optical center, would be a more appropriate candidate (see discussion below).[14,18,31] The advantages of using FPEG substitution on the **18**, SB-13, core, are readily modulating the lipohilicity, maintaining the neutrality, and providing a simple labeling for $^{18}$F by a nucleophilic substitution.[31]

To modulate the lipophilicity of $^{18}$F labeled stilbene (**20**, Figure 3), adding a short length of polyethylene glycol (PEG, $n$ = 2−12) and capping the end of the ethylene glycol chain with a fluorine atom was successfully employed.[17,31] In this series of compounds, **20**, $n$ = 2−12, the $^{18}$F is linked to the stilbene through a PEG chain, in which the number of PEG groups ranges from 2 to 12. The PEG groups were added to control lipophilicity, maintain the molecular neutrality, and improve bioavailability. The resulting FPEG derivatives, **20**, displayed excellent A$\beta$-binding affinities and high brain penetrations (Figure 3). A structure-binding-activity study of attaching a varying chain length FPEG ($n$ = 2−12) to these molecules for labeling with $^{18}$F showed that up to $n$ = 8, the $K_i$ was <10 nM. The lipophilicity does not change greatly between log $P$ of 2−3. However, surprisingly, the in vivo biodistribution studies in normal mice showed that when $n > 5$, there was a dramatic drop-off in brain penetration (see red boxes in Figure 3B). The finding is surprising and unexpected because the molecular weight for **20** ($n$ = 6) is 490, below the commonly accepted cut-off point (MW = 600) for penetration of intact blood−brain barrier.[32] It is likely that molecular size is only one of the factors controlling brain penetration of small and neutral molecules.[33] The flexible and polar FPEG chain may also interfere and limit brain penetration.

On the basis of the results of this structure−activity study, it was decided that **20**, where $n$ = 3, is sufficiently neutral, small, and lipophilic (this ligand is equivalent to **9**, BAY 94-9172 (AV-1). It provides an excellent combination of in vitro and in vivo properties for A$\beta$ plaque labeling, leading to desired characteristics suitable for in vivo imaging agents. The desirable properties include (1) high in vitro binding affinity ($K_i$ < 10 nM), (2) in vitro labeling of post-mortem human brain tissue sections displaying excellent labeling of A$\beta$ plaques, (3) very high in vivo brain penetration and fast washout from normal brain regions, (4) high ex vivo labeling of A$\beta$ plaque labeling in transgenic mice and excellent PET images in normal primate brain (high penetration and fast washout from normal regions), (5) low toxicity in normal animal models, and (6) efficient $^{18}$F labeling procedure adaptable for automated synthesis of PET tracers under a cGMP manufacturing condition (this requirement is particularly important because the half-life of $^{18}$F is 110 min; therefore, there is a time-constraint on making the final drug product for regional distribution).

It was reported that [$^{18}$F]Bay 94-9172 (AV1), **9**, is a useful in vivo imaging agent for targeting A$\beta$ plaques in the living human brain (Figure 4).[35] The preliminary clinical data from [$^{18}$F]Bay 94-9172 (AV1), **20** ($n$ = 3) or **9**, showed great promise as a PET imaging agent for detecting A$\beta$ plaques in the living human brain (Figure 4). The optimal signal-to-noise ratio was

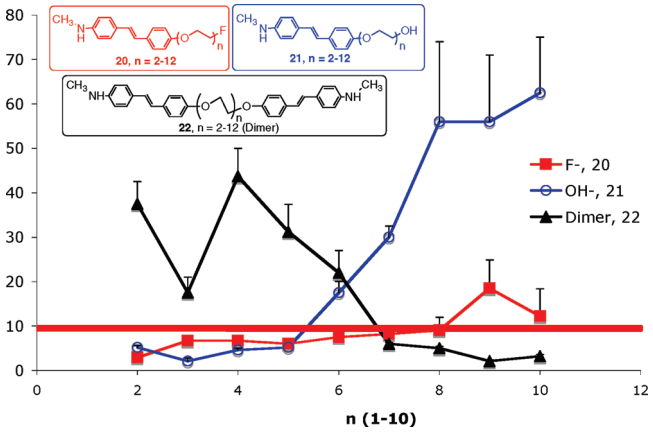


**Figure 5.** Inhibition constants ($K_i$, nM) of stilbene derivatives: fluoro monomer, **20**, hydroxyl monomer, **21**, and dimer, **22**. The $K_i$ values were measured by using [$^{125}$I]IMPY as the ligand and cortex homogenates of post-mortem AD brain ($K_i$ values of fluoro monomer, **20**, are shown in Figure 2). The red line indicates the $K_i$ value at 10 nM. It is important to note that for the dimer, **22**, the binding affinity increases dramatically when $n > 6$.

reached at 70−90 min after iv injection. This agent is now under a phase II clinical trial with the ultimate goal of using PET imaging to correlate the A$\beta$-plaque burden in living human brain.

### Monomers and Dimers of Stilbene Derivatives: Possible Binding Sites on A$\beta$ Aggregates

On the basis of the competition binding data (Figure 5) for the monomeric and dimeric stilbenes to the A$\beta$ plaques in AD brain homogenates, it is reasonable to summarize the following observation: there are likely to be multiple binding sites on the A$\beta$ aggregates of AD brain homogenates. The binding sites may be relatively flat. For the monovalent ligands, when $n > 5$, the binding affinity is reduced significantly, suggesting that the long PEG tail may interfere with the binding. Compounds with a hydroxyl group, **21**, are less tolerated than those end-capped with a fluorine atom, **20**. For the bivalent ligand (the dimeric stilbene derivatives, **22**) the length of the PEG chain is highly important; when the stilbene binding moieties are separated by $n > 7$, the binding affinity increases dramatically. The binding sites for stilbenes appear to be at least 6 units of PEG apart; the dimeric analogue, **22**, with $n > 6$ display a very dramatic increase of binding affinity (Figure 5).

The effect of increasing the PEG scaffold length on the binding of these monovalent and bivalent ligands to anti-DNP IgE in solution has been reported. Effects of multivalent binding sites vs linker length of an intramolecular protein−ligand system also suggested that the relationship may be useful for designing high binding affinity ligands.[36] The use of synthetic multivalent ligands to characterize receptor function on cell surfaces for signal transduction has recently been reported.[37] The data presented on the dramatic changes of binding affinity between dimers and monomers of stilbene derivatives may be useful in future studies on the binding pocket(s) of A$\beta$ plaques. It is important to note that the aggregated A$\beta$ peptides (predominantly 1−40 and 1−42) in AD are not designed by nature for any known biological functions. A$\beta$ plaques may not be useful for the purpose of any signal transduction mechanisms. However, the binding data in Figure 5 may suggest a unique arrangement of the presumed $\beta$-sheet formation of A$\beta$ aggregates. It is likely that a repeated $\beta$-sheet may also support the existence of repeated binding pockets on these aggregates.

### Development of [$^{18}$F]AV-45

To make the PET agent more efficient and faster in reaching high signal-to-noise ratio, [$^{18}$F]**10**, AV-45, was considered as the next candidate. Several critical and competing factors, such as brain penetration (initial brain uptake), washout from normal brain regions, in vivo metabolism, and the optimal time for achieving highest target-to-nontarget ratio were contemplated (Kung et al. *J. Nucl. Med.*, in press). This candidate was chosen from four different, but chemically closely related, styrylpyridine analogues.[14,38,39] All of these $^{18}$F agents have more or less met the criteria used for the development of **9**, BAY 94-9172 (AV-1): (1) high binding affinity to A$\beta$ aggregates ($K_i$ < 10 nM; (2) high binding selectivity ($K_i$ for other sites, > 100-fold; of particular importance is that there is no tau binding); (3) easily labeled with $^{18}$F for imaging; the radiochemical yields for preparation of AV-1 and AV-45 range from 20% to 35%, which is suitable for commercial scale production and distribution; (4) molecules that are small (MW < 500), lipophilic (measured log $P$ = 0.1−3.5), and neutral; (5) good initial brain uptake and desirable pharmacokinetics (high initial uptake of > 6.0% dose/g at 2 min after iv injection and fast washout at 30 min, less than 30% of initial uptake remaining in the brain of normal mice); (6) high brain uptake and fast washout in primate brain by PET imaging. It was found that when the stilbene of **9**, BAY 94-9172 (AV-1), is replaced by a styrylpyridine, lipophilicity is reduced further. From a series of styrylpyridine derivatives, **10**, AV-45, and **25**, AV-19, were selected.[14] Additional modification of the core structure has led to the preparation and testing of 1, 2-diphylacetylene (**23**, AV-138) or 1-phenyl-3-pyridinylacetylene (**24**, AV-144) derivatives.[38,40]

Initial clinical trial of [$^{18}$F]**25**, AV-19, suggested that the brain uptake was lower than expected, and this is likely due to a rapid in vivo metabolism of N-demethylation. Monodemethylation of [$^{18}$F]**25**, AV-19, led to the formation of [$^{18}$F]**10**, AV-45, which exhibits excellent brain uptake and washout in humans. Three candidates (**10**, AV-45; **23**, AV-138; and **24**, AV-144) showed the desired properties in humans (Figure 6). However, [$^{18}$F]**10**, AV-45, exhibited faster brain kinetics. The signal-to-noise ratio in the brain reaches an optimal level in 40−60 min after iv injection. Therefore, it is technically easier for performing PET imaging of AD patients. The selection of this final candidate, [$^{18}$F]**10**, AV-45, was facilitated by a newly introduced mechanism, exploratory investigative new drug application (eIND), by the FDA. The eIND permits the testing of structurally related new drugs in a limited number of human subjects (usually < 30 each) with one toxicology package. However, as the name has indicated, eIND is for exploratory clinical trial only; when the drug candidate(s) show promising results, a full IND will be needed for any commercial development. Using this mechanism, Avid Radiopharmaceuticals, Inc., successfully tested four new candidates. The eIND has expedited the preliminary testing of new PET tracers in a limited number of patients rapidly. A full IND for commercial development of [$^{18}$F]**10**, AV-45, had been filled, and currently, it is under a phase III clinical trial.

While A$\beta$-plaque deposition as visualized with **10**, [$^{18}$F]AV-45, is typically severe and widespread in AD subjects

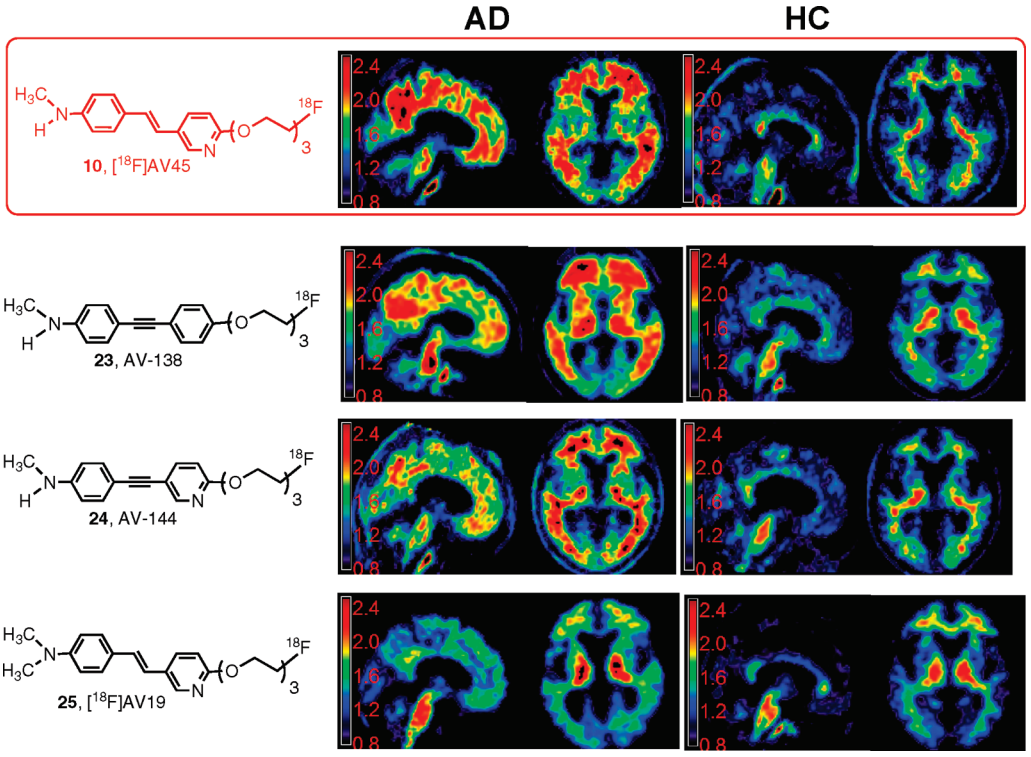


**Figure 6.** Comparative studies of four $^{18}$F PET imaging agents (**10**, AV-45; **23**, AV-138; **24**, AV-144; and **25**, AV-19) targeting A$\beta$ plaques in living human brain: AD (Alzheimer's disease); HC (healthy control). The scale for the *Y* axis represents SUV value. By visual inspection one can easily translate the specific vs nonspecific binding ratio in different regions of the brain. Three PET imaging tracers (**10**, AV-45; **23**, AV-138; and **24**, AV-144) displayed the desired properties for detecting A$\beta$ plaques in the brain of AD patients. One final candidate, **10**, AV-45, was selected for commercial development.

(Figure 6), deposition of varying degrees is also frequently seen in cognitively intact controls imaged with **10**, [$^{18}$F]AV-45. This may represent an early stage of presymptomatic AD. One of the major focuses of the phase III clinical trial is to establish a direct correlation between the PET imaging signals with post-mortem measurement of A$\beta$ plaque-burden in the brain of AD patients (see discussion below). It will be very important to determine the detection limit of A$\beta$ plaque-burden in the brain and the consistency of repeated PET imaging studies.

## Potential Clinical Utility of Detecting A$\beta$ Plaques in the Brain by PET Imaging

Many older patients may suffer symptoms of dementia (loss of memory); it is known that not all dementia patients have AD. The definitive diagnosis of AD requires confirmation of senile plaques in the post-mortem brain. Differential diagnosis in the clinics represents a formidable challenge even for the most experienced neurologists. The PET imaging of A$\beta$ plaques in the brain of dementia patients may have the following potential applications: (1) excluding plaque-negative patients with memory impairment from inappropriately receiving a diagnosis of AD; (2) assessing risk for AD or progression to AD in patients who are amyloid plaque-positive; (3) selecting patients for therapy and monitoring response to therapy for experimental therapeutics designed to target amyloid pathology.

One of the major confounding issues on the diagnosis of AD is the differentiation between normal aging and actual pathological neurodegeneration. It is often observed that normal aging is associated with some impairment of memory (dementia). Particularly for a patient with mild cognitive impairment (MCI), it is critical to determine if the MCI subject will eventually develop AD. Recently, **4**, [$^{11}$C]PIB, has been used in testing the association of A$\beta$ plaque-burden in the brain of patients with MCI and prevalence of conversion from MCI to AD. By use of PIB/PET to study the relationship between A$\beta$ plaque burden and AD neurological measurements, the results seem to suggest that there are some MCI cases that convert to AD while those with lower PIB uptake in the cortex appear to have less propensity to convert to AD.[20] These reports of using PET imaging in testing AD patients and of patients with MCI have generated the exciting possibility that such a procedure may be useful in differential diagnosis and monitoring patients showing apparent lapse of memory. Indeed, [$^{18}$F]AV-45 is already being used in a large number of therapeutic trials, both to assess pretreatment levels of A$\beta$ plaques (presumably predicting those patients that are more likely to respond to A$\beta$ plaque-targeted therapies) and to monitor response to treatment (in the case of therapeutics aimed at lowering amyloid plaque burden). The phase III clinical trial of **10**, [$^{18}$F]AV-45, is to establish the relationship between measurements of A$\beta$ plaques in the brain using PET imaging and true levels of amyloid burden assessed by histology at autopsy. With the introduction of **10**, [$^{18}$F]AV-45, it may be feasible to achieve a widespread application benefiting a large number of older patients.

In summary, currently there are three $^{18}$F tracers targeting A$\beta$ aggregates (**8**, GE-067; **9**, BAY 94-9172; and **10**, AV-45) that are in active commercial development. Two candidates, a stilbene derivative ([$^{18}$F]**9**, BAY 94-9172,) and a styrylpyridine ([$^{18}$F]**10**, AV-45), are related PET imaging agents containing an end-capped fluoropolyethylene glycol side chain (FPEG); both agents have shown promising results in clinical trials.

These new PET imaging agents may lead to highly anticipated advances in diagnosis and treatment of Alzheimer's disease (AD).

## Epilogue

"Talent hits a target no one else can hit; Genius hits a target no one else can see." This quote is from Arthur Schopenhauer, a 19th century German philosopher known for his atheistic pessimism and philosophical clarity.

It is sobering to reflect on the fact that 100 years have passed since Dr. Alois Alzheimer first reported the association between A$\beta$ plaques in the brain and the disease that bears his name. It is also humbling to recognize that several PET imaging agents finally can hit this known target a century later. One may wonder how many geniuses are out there who may advance the field by hitting other targets important for Alzheimer's disease (AD) that no one has yet seen.

**Acknowledgment.** This work was partially supported by grants awarded from the National Institutes of Health (Grant ROI-AG-022559 to H.F.K. and Grant R43AG032206, D.S.). The authors thank Dr. Mei-Ping Kung for providing part of the binding data and Catherine Hou for helpful editorial assistance.

## Biographies

**Hank F. Kung** was educated as a medicinal chemist in the Department of Medicinal Chemistry, School of Pharmacy, SUNY Buffalo, NY. After postdoctoral training under Dr. Monte Blau at Roswell Park Memorial Institute, Dr. Kung joined the Department of Nuclear Medicine, SUNY Buffalo, NY. He moved to the Department of Radiology, University of Pennsylvania, in 1987. He is well-known for his work in developing new radiopharmaceuticals for brain imaging in conjunction with single photon emission computed tomography (SPECT) and positron emission tomography (PET). Many of the new radiopharmaceuticals for mapping brain functions have been developed in his laboratory and tested in humans. Together with Dr. Daniel Skovronsky, Avid Radiopharmaceuticals, Inc., was founded in 2004.

**Seok Rye Choi** received her Ph.D. degree in Radiopharmaceutical Chemistry from Kyoto University under Professor Yokoyama. In 1998−2006, she worked as a postdoctoral fellow and later as a research associate in Dr. Kung's lab at University of Pennsylvania. Since 2006, she has been a Senior Pharmacologist at Avid Radiopharmaceuticals. Her research interests are focused on the development of imaging agents of neurodegenerative diseases.

**Wenchao Qu** received his B.S. and M.S. from Nanjing University of Science and Technology, China, in 1992 and 1999, respectively. He then earned his Ph.D. degree in Organic Chemistry at The University of Akron, OH, in 2006 under the direction of Professor Michael J. Taschner. After two-and-a-half years' postdoctoral research training under the mentorship of Professor Hank F. Kung, he was appointed as a Research Assistant Professor at the Department of Radiology, University of Pennsylvania, in July, 2008. Currently, he is focusing on synthesizing isotope labeled bioactive organic molecules and further evaluating them as probes for imaging and diagnosis of various diseases. In addition, he is also interested in developing new fluorination methodologies that are practical and useful in pharmaceutical chemistry.

**Wei Zhang** received his Ph.D. in Chemistry from Rutgers, the State University of New Jersey, Newark. During his postdoctoral training under Dr. Hank F. Kung at University of Pennsylvania, he was one of the key members in developing PET imaging agents targeting amyloid plaques in human brain. After that he joined Avid Radiopharmaceuticals as a Senior Research Chemist focusing on the process development for new radiopharmaceuticals.

**Daniel Skovronsky** is the founder and CEO of Avid Radiopharmaceuticals, a biotechnology company focused on the development of novel molecular imaging agents. Dr. Skovronsky trained as a resident in Pathology and completed a fellowship in Neuropathology at the Hospital of the University of Pennsylvania. Dr. Skovronsky received his M.D. and Ph.D. from the University of Pennsylvania and did his undergraduate training in molecular biochemistry at Yale University.

## References

(1) Burns, A.; Iliffe, S. Alzheimer's disease. *Br. Med. J.* **2009**, *338*, b158.
(2) Roberson, E. D.; Mucke, L. 100 years and counting: prospects for defeating Alzheimer's disease. *Science* **2006**, *314*, 781–784.
(3) Hardy, J.; Selkoe, D. J. The amyloid hypothesis of Alzheimer's disease: progress and problems on the road to therapeutics. *Science* **2002**, *297*, 353–356.
(4) Sperling, R. A.; Laviolette, P. S.; O'Keefe, K.; O'Brien, J.; Rentz, D. M.; Pihlajamaki, M.; Marshall, G.; Hyman, B. T.; Selkoe, D. J.; Hedden, T.; Buckner, R. L.; Becker, J. A.; Johnson, K. A. Amyloid deposition is associated with impaired default network function in older persons without dementia. *Neuron* **2009**, *63*, 178–188.
(5) Jakob-Roetne, R.; Jacobsen, H. Alzheimer's disease: from pathology to therapeutic approaches. *Angew. Chem., Int. Ed.* **2009**, *48*, 3030–3059.
(6) Knopman, D. S.; DeKosky, S. T.; Cummings, J. L.; Chui, H.; Corey-Bloom, J.; Relkin, N.; Small, G. W.; Miller, B.; Stevens, J. C. Practice parameter: diagnosis of dementia (an evidence-based review). Report of the Quality Standards Subcommittee of the American Academy of Neurology. *Neurology* **2001**, *56*, 1143–1153.
(7) Lopponen, M.; Raiha, I.; Isoaho, R.; Vahlberg, T.; Kivela, S. L. Diagnosing cognitive impairment and dementia in primary health care − a more active approach is needed. *Age Ageing* **2003**, *32*, 606–612.
(8) Minoshima, S. Imaging Alzheimer's disease: clinical applications. *Neuroimaging Clin. North Am.* **2003**, *13*, 769–780.
(9) Mosconi, L.; Tsui, W. H.; Herholz, K.; Pupi, A.; Drzezga, A.; Lucignani, G.; Reiman, E. M.; Holthoff, V.; Kalbe, E.; Sorbi, S.; Diehl-Schmid, J.; Perneczky, R.; Clerici, F.; Caselli, R.; Beuthien-Baumann, B.; Kurz, A.; Minoshima, S.; de Leon, M. J. Multicenter standardized $^{18}$F-FDG PET diagnosis of mild cognitive impairment, Alzheimer's disease, and other dementias. *J. Nucl. Med.* **2008**, *49*, 390–398.
(10) Mathis, C. A.; Wang, Y.; Klunk, W. E. Imaging b-amyloid plaques and neurofibrillary tangles in the aging human brain. *Curr. Pharm. Des.* **2004**, *10*, 1469–1492.
(11) Henriksen, G.; Yousefi, B. H.; Drzezga, A.; Wester, H. J. Development and evaluation of compounds for imaging of beta-amyloid plaque by means of positron emission tomography. *Eur. J. Nucl. Med. Mol. Imaging* **2008**, *35*, S75–81.
(12) Barrio, J. R.; Satyamurthy, N.; Huang, S. C.; Petric, A.; Small, G. W.; Kepe, V. Dissecting molecular mechanisms in the living brain of dementia patients. *Acc. Chem. Res.* **2009**, *42*, 842–850.
(13) Kung, H. F.; Lee, C.-W.; Zhuang, Z. P.; Kung, M. P.; Hou, C.; Plossl, K. Novel stilbenes as probes for amyloid plaques. *J. Am. Chem. Soc.* **2001**, *123*, 12740–12741.
(14) Zhang, W.; Kung, M. P.; Oya, S.; Hou, C.; Kung, H. F. (18) F-Labeled styrylpyridines as PET agents for amyloid plaque imaging. *Nucl. Med. Biol.* **2007**, *34*, 89–97.
(15) Mathis, C. A.; Wang, Y.; Holt, D. P.; Huang, G.-F.; Debnath, M. L.; Klunk, W. E. Synthesis and evaluation of $^{11}$C-labeled 6-substituted 2-arylbenzothiazoles as amyloid imaging agents. *J. Med. Chem.* **2003**, *46*, 2740–2754.
(16) Eckelman, W. C.; Mathis, C. A. Targeting proteins in vivo: in vitro guidelines. *Nucl. Med. Biol.* **2006**, *33*, 161–164.
(17) Zhang, W.; Oya, S.; Kung, M. P.; Hou, C.; Maier, D. L.; Kung, H. F. F-18 PEG stilbenes as PET imaging agents targeting A$\beta$ aggregates in the brain. *Nucl. Med. Biol.* **2005**, *32*, 799–809.
(18) Zhang, W.; Oya, S.; Kung, M. P.; Hou, C.; Maier, D. L.; Kung, H. F. F-18 stilbenes as PET imaging agents for detecting beta-amyloid plaques in the brain. *J. Med. Chem.* **2005**, *48*, 5980–5988.
(19) Klunk, W. E.; Debnath, M. L.; Pettegrew, J. W. Small-molecule beta-amyloid probes which distinguish homogenates of Alzheimer's and control brains. *Biol. Psychiatry* **1994**, *35*, 627.
(20) Rowe, C. C.; Ng, S.; Ackermann, U.; Gong, S. J.; Pike, K.; Savage, G.; Cowie, T. F.; Dickinson, K. L.; Maruff, P.; Darby, D.; Smith, C.; Woodward, M.; Merory, J.; Tochon-Danguy, H.; O'Keefe, G.;

Klunk, W. E.; Mathis, C. A.; Price, J. C.; Masters, C. L.; Villemagne, V. L. Imaging beta-amyloid burden in aging and dementia. *Neurology* **2007**, *68*, 1718–1725.
(21) Johnson, A. E.; Jeppsson, F.; Sandell, J.; Wensbo, D.; Neelissen, J. A.; Jureus, A.; Strom, P.; Norman, H.; Farde, L.; Svensson, S. P. AZD2184: a radioligand for sensitive detection of beta-amyloid deposits. *J. Neurochem.* **2009**, *108*, 1177–1186.
(22) Choi, S. R.; Golding, G.; Zhuang, Z.; Zhang, W.; Lim, N.; Hefti, F.; Benedum, T. E.; Kilbourn, M. R.; Skovronsky, D.; Kung, H. F. Preclinical properties of 18F-AV-45: a PET imaging agent for A$\beta$ plaques in the brain. *J. Nucl. Med.*, in press.
(23) Koole, M.; Lewis, D. M.; Buckley, C.; Nelissen, N.; Vandenbulcke, M.; Brooks, D. J.; Vandenberghe, R.; Van Laere, K. Whole-body biodistribution and radiation dosimetry of $^{18}$F-GE067: a radioligand for in vivo brain amyloid imaging. *J. Nucl. Med.* **2009**, *50*, 818–822.
(24) Maya, Y.; Ono, M.; Watanabe, H.; Haratake, M.; Saji, H.; Nakayama, M. Novel radioiodinated aurones as probes for SPECT imaging of beta-amyloid plaques in the brain. *Bioconjugate Chem.* **2009**, *20*, 95–101.
(25) Kung, M. P.; Zhuang, Z. P.; Hou, C.; Kung, H. F. Development and evaluation of iodinated tracers targeting amyloid plaques for SPECT imaging. *J. Mol. Neurosci.* **2004**, *24*, 49–53.
(26) Newberg, A. B.; Wintering, N. A.; Plossl, K.; Hochold, J.; Stabin, M. G.; Watson, M.; Skovronsky, D.; Clark, C. M.; Kung, M. P.; Kung, H. F. Safety, biodistribution, and dosimetry of $^{123}$I-IMPY: a novel amyloid plaque-imaging agent for the diagnosis of Alzheimer's disease. *J. Nucl. Med.* **2006**, *47*, 748–754.
(27) Qu, W.; Kung, M. P.; Hou, C.; Benedum, T. E.; Kung, H. F. Novel styrylpyridines as probes for SPECT imaging of amyloid plaques. *J. Med. Chem.* **2007**, *50*, 2157–2165.
(28) Ono, M.; Haratake, M.; Nakayama, M.; Kaneko, Y.; Kawabata, K.; Mori, H.; Kung, M. P.; Kung, H. F. Synthesis and biological evaluation of (*E*)-3-styrylpyridine derivatives as amyloid imaging agents for Alzheimer's disease. *Nucl. Med. Biol.* **2005**, *32*, 329–335.
(29) Verhoeff, N. P.; Wilson, A. A.; Takeshita, S.; Trop, L.; Hussey, D.; Singh, K.; Kung, H. F.; Kung, M.-P.; Houle, S. In vivo imaging of Alzheimer disease beta-amyloid with [$^{11}$C]SB-13 PET. *Am. J. Geriatr. Psychiatry* **2004**, *12*, 584–595.
(30) Kung, M.-P.; Hou, C.; Zhuang, Z.-P.; Skovronsky, D.; Kung, H. F. Binding of two potential imaging agents targeting amyloid plaques in postmortem brain tissues of patients with Alzheimer's disease. *Brain Res.* **2004**, *1025*, 89–105.
(31) Stephenson, K. A.; Chandra, R.; Zhuang, Z. P.; Hou, C.; Oya, S.; Kung, M. P.; Kung, H. F. Fluoro-pegylated (FPEG) imaging agents targeting Abeta aggregates. *Bioconjugate Chem.* **2007**, *18*, 238–246.
(32) Dischino, D. D.; Welch, M. J.; Kilbourn, M. R.; et al. Relationship between lipophicility and brain extraction of C-11 labeled radiopharmaceuticals. *J. Nucl. Med.* **1983**, *24*, 1030–1038.
(33) Pardridge, W. M. Molecular biology of the blood−brain barrier. *Mol. Biotechnol.* **2005**, *30*, 57–70.
(34) Zhuang, Z. P.; Kung, M. P.; Wilson, A.; Lee, C. W.; Plossl, K.; Hou, C.; Holtzman, D. M.; Kung, H. F. Structure−activity relationship of imidazo[1,2-*a*]pyridines as ligands for detecting beta-amyloid plaques in the brain. *J. Med. Chem.* **2003**, *46*, 237–243.
(35) Rowe, C. C.; Ackerman, U.; Browne, W.; Mulligan, R.; Pike, K. L.; O'Keefe, G.; Tochon-Danguy, H.; Chan, G.; Berlangieri, S. U.; Jones, G.; Dickinson-Rowe, K. L.; Kung, H. P.; Zhang, W.; Kung, M. P.; Skovronsky, D.; Dyrks, T.; Holl, G.; Krause, S.; Friebe, M.; Lehman, L.; Lindemann, S.; Dinkelborg, L. M.; Masters, C. L.; Villemagne, V. L. Imaging of amyloid beta in Alzheimer's disease with (18)F-BAY94-9172, a novel PET tracer: proof of mechanism. *Lancet Neurol.* **2008**, *7*, 129–135.
(36) Krishnamurthy, V. M.; Semetey, V.; Bracher, P. J.; Shen, N.; Whitesides, G. M. Dependence of effective molarity on linker length for an intramolecular protein−ligand system. *J. Am. Chem. Soc.* **2007**, *129*, 1312–1320.
(37) Kiessling, L. L.; Gestwicki, J. E.; Strong, L. E. Synthetic multivalent ligands as probes of signal transduction. *Angew. Chem., Int. Ed.* **2006**, *45*, 2348–2368.
(38) Chandra, R.; Oya, S.; Kung, M. P.; Hou, C.; Jin, L. W.; Kung, H. F. New diphenylacetylenes as probes for positron emission tomographic imaging of amyloid plaques. *J. Med. Chem.* **2007**, *50*, 2415–2423.
(39) Skovronsky, D. B.; Coleman, R. E.; Frey, K.; Garg, P. K.; Ichise, M.; Lowe, V. J.; Mintum, M.; Wong, D. F.; Kung, H. F. Results of multi-center, multi-ligand clinical trials with five $^{18}$F-labeled amyloid-imaging agents in Alzheimer's disease patients and healthy elderly controls. *J. Nucl. Med.* **2008**, *49*, 34 pp.
(40) Qu, W.; Kung, M. P.; Hou, C.; Oya, S.; Kung, H. F. Quick assembly of 1,4-diphenyltriazoles as probes targeting beta-amyloid aggregates in Alzheimer's disease. *J. Med. Chem.* **2007**, *50*, 3380–3387.